

STA-FEM: Exact Streaming Assembly for Preplanned Dynamic Tetrahedral Topology Edits

MANISH ACHARYA, Vanderbilt University, USA
DAVID HYDE, Vanderbilt University, USA

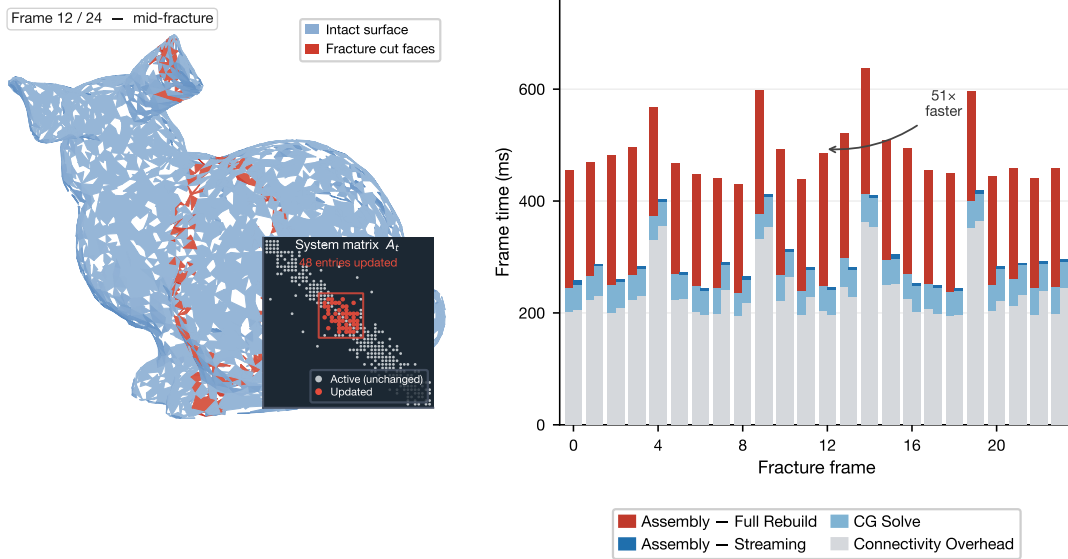


Fig. 1. **Streaming assembly on a fracture sequence.** *Left:* Surface mesh at frame 12 of a 24-frame fracture sequence; red faces mark newly introduced cut geometry; the inset shows the sparse system matrix A_t with only 48 entries updated by the streaming pass (vs. a full rebuild of thousands). *Right:* Per-frame cost breakdown comparing full rebuild to streaming update. The streaming assembly cost (dark blue) is negligible relative to the CG solve and connectivity overhead shared by both methods, yielding a 51 \times assembly speedup at peak fracture.

Dynamic tetrahedral simulation pipelines rebuild topology-dependent solver state after every fracture, refinement, or merge event—discarding structural continuity that survives each edit and spending global work on what are often local changes. We present STA-FEM, a streaming assembly method for simulations with topologically-dynamic tetrahedral meshes operating on a fixed superset mesh: when the candidate element pool is preallocated and the per-frame edit stream is exposed, the surrounding solver, preconditioner, and time-stepping layers stay unchanged while the per-frame assembly step is replaced with persistent incremental updates that match a full-rebuild approach exactly at every frame. Across various three-dimensional examples with up to 460k elements, the method delivers end-to-end speedups of 1.37 \times to 1.61 \times over full-rebuild with orders-of-magnitude reductions in matrix update cost, preserving exact matrix parity in all tested frames against a stronger exact *local recomputation* baseline. We test our algorithm in realistic fracture simulation pipelines and observe up to 76% speedups in fracture frame time with exact equivalence to a ground-truth full-rebuild algorithm. These results establish exact streaming assembly as a potentially practical approach for simulating tetrahedral meshes with dynamic topology.

CCS Concepts: • **Computing methodologies** → **Simulation types and techniques**; **Physics-based simulation**.

Additional Key Words and Phrases: dynamic topology, tetrahedral meshes, incremental updates, FEM, sparse linear systems, simulation systems

Authors' Contact Information: Manish Acharya, Vanderbilt University, USA, manish.acharya@vanderbilt.edu; David Hyde, Vanderbilt University, USA, david.hyde.1@vanderbilt.edu.

1 Introduction

Tetrahedral meshes with dynamic topology are common in computer graphics, such as in fracture simulations. These meshes may have tetrahedra removed during fracture and may undergo refinement (coarse elements replaced by preallocated children) and merge (separated regions reconnected) operations [Molino et al. 2004; O'Brien and Hodgins 1999; Wicke et al. 2010]. In ordinary tetrahedral pipelines, each such edit still triggers a full solver-side rebuild of the system matrix before the next solve, which—while simple—discards structural continuity surviving the edit and spends global work on what are often local changes.

In many cases, when simulating a dynamic tetrahedral mesh, its potential future topological states may be known ahead of time. For instance, when an object is pre-fractured along Voronoi or stress-aligned partitions and then simulated, the fragment boundaries are fixed, and the simulation simply decides which elements separate and when (along with geometric deformations that do not affect topology) [Müller et al. 2013; Sellán et al. 2023]. As another example, papers such as Koschier et al. [2014] pre-generate refinement hierarchies (i.e., every coarse tetrahedron has a known set of potential children), meaning this superset of potential mesh elements is known a priori. This property is enjoyed by various adaptive mesh refinement strategies [Arnold et al. 2000; Kossaczky 1994; Maubach

1995; Mitchell 2016]. Lastly, in surgical simulation, one may know the set of elements that could be merged, but the timing and order is driven by simulation [Bielser et al. 2003; Molino et al. 2004]. We call simulations *preplanned* when the potential topological states of a tetrahedral mesh may be allocated ahead of running a simulation.

This paper investigates the following question: for preplanned simulations with dynamic tetrahedral topologies, can the simulation loop preserve solver-side structural continuity across local topology edits and obtain meaningful end-to-end savings without changing the surrounding solve loop? Our proposed method, STA-FEM, answers this question in the affirmative. We find that topology-dependent sparse operators can be maintained *exactly* under tetrahedral edit streams, and that exact maintained-assembly view is strong enough to outperform both global rebuild and exact touched-region recomputation. The method is designed as a narrow integration point inside an existing implicit solver: given the same edit stream, solver, preconditioner, and timestepper—and provided the pipeline operates on a fixed superset mesh—STA-FEM replaces only rebuild-oriented topology-dependent assembly.

The key idea of our method is to treat topology edits as a streaming event sequence and update only the matrix entries affected by changed tetrahedra. Rather than recomputing the full matrix graph after each event, the method maintains persistent hidden state and updates only touched matrix entries. In the main proxy system, this hidden state is edge multiplicity, which determines exact binary edge activity. In an additional transfer study, the same event-driven policy maintains a true element-assembled vector-valued linear-elasticity operator [Sifakis and Barbič 2012]. This also lets us distinguish two exact alternatives: a stronger *local recomputation* baseline that rescans only candidate entries touched by the event, and the proposed *persistent streaming* policy that keeps maintained state across frames.

We offer several numerical experiments in support of STA-FEM. A vector-valued linear-tetrahedron elasticity operator study shows the proposed maintenance pattern works on a block-structured FEM operator; the implicit Euler dynamic loop shows the benefit persists in a practical simulation context. A multi-model proxy suite establishes broad dynamic-topology behavior across four objects and three scenarios; the exact `local_recompute` baseline shows the method outperforms a legitimate exact alternative. Additionally, a temporal-locality diagnostic identifies when persistent maintained state is most valuable over exact local rescanning.

Our main contributions are:

- an exact streaming matrix-maintenance method for dynamic tetrahedral edit sequences in a preplanned simulation (i.e., on a fixed superset mesh), validated on a linear elasticity operator and an implicit Euler dynamic loop;
- an event-driven benchmark pipeline covering fracture, refinement, and merge under matched schedules and metrics;
- a reproducible quantitative and visual evaluation across various 3D test meshes [Cutler et al. 2004], comparing STA-FEM against full-rebuild and local-recomputation baselines.

To encourage reproducibility and adoption, complete source code is attached to the submission and will be released under the NCSA open-source license upon publication.

2 Related Work

2.1 Dynamic Topology in Mesh-Based Simulation

Topology change has long been a core challenge in physically-based animation. O’Brien and Hodgins [1999] showed how fracture can be driven by stress analysis over volumetric meshes, while Molino et al. [2004] addressed more general cutting and separation through a virtual-node formulation. Wicke et al. [2010] later demonstrated that local remeshing can be integrated into elastoplastic simulation loops without globally replacing the entire mesh. Koschier et al. [2014] introduced a reversible tetrahedral refinement scheme for brittle fracture that preserves mesh quality through local topological operations—exemplifying the kind of preallocated refinement hierarchy STA-FEM exploits. Hahn and Wojtan [2015] pursued boundary-element formulations of brittle fracture for high-resolution surfaces. More recently, Ferguson et al. [2023] showed that remeshing can occur within a single timestep for contacting elastodynamics, while Fan et al. [2022] extended brittle fracture simulation to material point methods; both highlight that topology changes mid-simulation remain an active area with ongoing solver-level challenges. STA-FEM is aligned with this line of work in that it targets changing tetrahedral topology, but its focus is narrower: incremental maintenance of topology-dependent solver structures for preplanned simulations.

2.2 Sparse Solver Maintenance

Our update rule is particularly motivated by the observation that problems involving sparse linear systems often benefit from local modification rather than repeated full reconstruction. Davis and Hager studied sparse Cholesky modification algorithms whose cost scales with the portion of the factorization that actually changes [Davis and Hager 1999], and CHOLMOD operationalized this update-oriented viewpoint in widely used sparse software [Chen et al. 2008]. More recently, Zarebavani et al. [2025] showed that Cholesky reordering itself can be reused adaptively when the sparsity pattern changes dynamically, directly extending the maintained-factorization idea to dynamic-topology settings.

Most directly related to STA-FEM, Yeung et al. [Yeung et al. 2020] introduced AMPS, which maintains FEM stiffness systems under real-time mesh cutting through augmented-matrix formulations and Schur-complement updates, avoiding full refactorization across topology changes. AMPS operates at the linear-system level, modifying the solved system via augmentation; STA-FEM operates one layer earlier by maintaining the assembled topology-dependent operator itself. The two ideas are complementary: an STA-FEM-maintained operator could in principle feed an AMPS-style augmentation layer, although we leave that integration to future work. STA-FEM does not update a Cholesky factorization directly either, but it adopts the same systems principle: preserve persistent sparse state and edit only the portion affected by local topology events.

2.3 Graph Streaming Algorithms

Treating per-frame topology edits as an event sequence connects naturally to graph streaming, a well-established model in which edits to a graph are processed as a sequence of edge insertions and deletions [McGregor 2014; Muthukrishnan 2005]. Graph streaming algorithms are appealing because they maintain quantities of interest using

sublinear space and incremental per-event work. For instance, the semi-streaming model of Feigenbaum et al. [2005] formalized the regime in which $O(n \text{ polylog } n)$ memory suffices for many graph problems on n -vertex graphs, while the linear-sketching framework of Ahn et al. [2012] showed that connectivity, spanning forests, and related structural properties admit small-space algorithms even under fully dynamic edge streams with deletions. Follow-on work has extended this line to spectral sparsifiers of graph Laplacians in dynamic streams [Kapralov et al. 2015] and to matchings [Chitnis et al. 2016].

STA-FEM is a domain-specific instance of this pattern, but the constraints of our setting differ from standard graph streaming problems in two ways. First, the maintained object is not a graph property but an assembled topology-dependent sparse operator itself, and it must be maintained *exactly*, not approximated, because downstream solvers consume it directly. Second, the streams are small per frame (tens to hundreds of edited tetrahedra, not millions of edges), so the relevant scarce resource is per-frame assembly time inside a fixed simulation loop rather than memory; STA-FEM’s state grows with the active mesh rather than polylogarithmically, and is therefore not a sublinear-space algorithm in the theoretical sense. What we adopt from the graph streaming literature is foremost its basic premise—to treat topology edits as a stream and update only what each event changes. The persistent-state benefit we demonstrate, with update cost scaling as $O(|\Delta_t|)$ rather than $O(|\mathcal{T}_t|)$, is the same type of advantage seen in other graph streaming algorithms.

3 Method

STA-FEM maintains a topology-dependent sparse operator under a stream of tetrahedral edits. The simulation loop is standard: at each frame, the system receives a set of deleted and added tetrahedra, updates whatever solver-side structures are topology-dependent, materializes the current matrix, and solves a linear system. Our contribution replaces only one component of that loop—the topology-dependent assembly step—with an exact streaming maintenance procedure that updates the matrix incrementally rather than reconstructing it.

The method takes three inputs. First, a fixed superset of vertex positions and a fixed candidate pool of tetrahedra: the maximal set of tetrahedra the simulation could ever activate, known up front but with the current active subset driven by the simulation. Second, a per-frame edit stream consisting of deleted and added tetrahedra. Third, an initial active mask. From these, STA-FEM maintains a small amount of persistent state—an active mask, an edge-multiplicity map, a degree vector, and the current sparse matrix—and updates it incrementally on each frame. The key invariant, established formally in Section 3.3, is that the maintained matrix is exactly equal to the matrix obtained by rebuilding from scratch on the current active tetrahedron set.

We instantiate this maintenance pattern on two operators in this paper. The first is a graph-Laplacian-based proxy whose sparsity is governed by tetrahedron-to-edge incidence; we use it for the broad multi-model evaluation (Section 6.3) because it isolates assembly-maintenance behavior cleanly without variability from constitutive

models or material parameters. The second is a vector-valued linear-tetrahedron elasticity operator assembled from per-element 12×12 stiffness blocks; this is a true element-assembled FEM operator and is the subject of the transfer study in Section 6.1. The maintenance machinery is the same in both cases; only the per-edge update rule differs (binary thresholding for the proxy, additive accumulation of element contributions for elasticity). In Sections 3.1–3.3, we discuss the method applied to the proxy operator since its update rule is simpler to state, and then we bridge to element-assembled operators in Section 3.4.

3.1 Problem Setup

For a given dynamic tetrahedral mesh, let $V \in \mathbb{R}^{n \times 3}$ denote the vertex positions of the superset of potential mesh vertices, and let \mathcal{T}_t be the active tetrahedron set at frame t —that is, the subset of the candidate pool currently contributing to the simulation, which the active mask tracks. Each active tetrahedron induces six undirected graph edges. We define an edge multiplicity function

$$c_t(u, v) = \sum_{\tau \in \mathcal{T}_t} \mathbf{1}[(u, v) \in E(\tau)] \quad (1)$$

that counts how many active tetrahedra an edge (u, v) contributes to at time t , where $E(\tau)$ is the set of the six undirected edges of tetrahedron τ .

Our proxy operator is built from *binary* edge activity

$$a_t(u, v) = \mathbf{1}[c_t(u, v) > 0]. \quad (2)$$

From these binary activities we form an unweighted graph Laplacian-like system

$$L_t(u, v) = \begin{cases} -a_t(u, v), & u \neq v, \\ \sum_{w \neq u} a_t(u, w), & u = v, \end{cases} \quad (3)$$

and use the stabilized system

$$A_t = L_t + \varepsilon I \quad (4)$$

with a small $\varepsilon > 0$. This is the matrix solved at each frame in the proxy setting.

We make two design comments. First, we pair a binary off-diagonal pattern with an explicitly maintained edge multiplicity c_t . The off-diagonal entries are determined by $a_t = \mathbf{1}[c_t > 0]$, but c_t itself is what the maintenance rule updates: tracking the multiplicity, not just the binary activity, is what lets us detect zero-to-nonzero transitions exactly under deletions without rescanning incident tetrahedra. Second, the proxy’s sparsity pattern is determined by the same tetrahedron-to-edge incidence that governs a true vector-valued elasticity operator, which is why the maintenance machinery transfers without modification to the elasticity setting in Section 3.4.

3.2 Streaming Matrix Update

Each frame receives two edit sets:

$$\Delta_t^- = \{\text{deleted tetrahedra on frame } t\}, \quad (5)$$

$$\Delta_t^+ = \{\text{added tetrahedra on frame } t\}. \quad (6)$$

These induce an edge-count update

$$c_{t+1}(e) = c_t(e) + \sum_{\tau \in \Delta_t^+} \mathbf{1}[e \in E(\tau)] - \sum_{\tau \in \Delta_t^-} \mathbf{1}[e \in E(\tau)]. \quad (7)$$

Rather than rebuild all matrix entries, STA-FEM visits only edges touched by tetrahedra in $\Delta_t = \Delta_t^- \cup \Delta_t^+$. Whenever an edge multiplicity flips between zero and nonzero, the corresponding off-diagonal entries are inserted or removed, and the two endpoint diagonal terms are updated. This converts a global rebuild into a local sparse maintenance step. In contrast to direct factor-update methods such as sparse Cholesky modification [Chen et al. 2008; Davis and Hager 1999] and to system-level augmentation methods such as AMPS [Yeung et al. 2020], we operate one layer earlier in the stack by updating the assembled topology-dependent system itself.

3.3 Maintained State and Exactness

Fracture and merge events toggle the active mask of existing tetrahedra; refinement events activate preallocated child tetrahedra and deactivate their parents. Under this model, STA-FEM maintains:

- an active mask over tetrahedra;
- precomputed tetrahedron-to-edge incidence;
- an edge-multiplicity map $c_t(e)$;
- a degree vector for diagonal entries;
- a sparse matrix representation storing the current active off-diagonal pattern and diagonal terms.

The key invariant is exact equivalence to a full-rebuild approach:

After every event sequence, the maintained matrix A_t equals the matrix obtained by rebuilding from scratch on the current active tetrahedron set.

This follows because each topology event changes only the multiplicities of edges incident to the edited tetrahedra. Edges whose multiplicity remains positive stay active, edges whose multiplicity drops to zero are removed, and edges whose multiplicity rises from zero are inserted. The diagonal degree terms are updated from the same transitions, so the maintained operator matches the rebuild operator exactly.

3.4 Bridge to Element-Assembled Operators

The same event-driven maintenance idea also applies to additive element assembly. For a fixed superset tetrahedral mesh, many scalar or block FEM systems can be written as

$$\tilde{A}_t = \sum_{\tau \in \mathcal{T}_t} P_\tau^T K^{(\tau)} P_\tau + \varepsilon I, \quad (8)$$

where $K^{(\tau)}$ is the local element matrix of tetrahedron τ and P_τ injects its local degrees of freedom into the global system [Sifakis and Barbič 2012]. Under a topology edit, only tetrahedra in Δ_t change membership in the sum. In the transfer experiment of Section 6.1, we instantiate $K^{(\tau)}$ as a standard vector-valued linear-tetrahedron elasticity matrix under fixed material parameters.

The same exactness argument (Section 3.3) carries over to additive element assembly, except that touched global entries are updated by adding or removing local element contributions rather than by thresholding binary edge activity.

3.5 Complexity Discussion

We consider three update policies in this work: `full_rebuild`, which reassembles the matrix from scratch on \mathcal{T}_t after every edit and serves as our reference baseline; `local_recompute`, an exact

policy that restricts attention to candidate entries touched by the current event but recomputes each from scratch by rescanning all incident active tetrahedra, with no maintained state carried across frames; and `streaming_update`, the proposed policy, which preserves the maintained state of Section 3.3 (edge multiplicities for the proxy operator, additive element contributions for the element-assembled operator of Section 3.4) and applies only the incremental deltas induced by each edit. All three produce identical matrices at every frame by construction; they differ only in how much state and rework each carries between frames:

PROPOSITION 1 (PER-FRAME UPDATE COST). *Let $|\mathcal{T}_t|$ be the number of active tetrahedra at time t , $|\Delta_t| = |\Delta_t^-| + |\Delta_t^+|$ the number of edited tetrahedra, and κ the maximum number of tetrahedra incident to any candidate edge or entry. Per-frame assembly update work satisfies:*

$$\begin{aligned} \text{full_rebuild} &: O(|\mathcal{T}_t|), \\ \text{local_recompute} &: O(|\Delta_t| \cdot \kappa), \\ \text{streaming_update} &: O(|\Delta_t|). \end{aligned}$$

For meshes with bounded valence and $|\Delta_t| \cdot \kappa \leq |\mathcal{T}_t|$, our proposed streaming update achieves the lowest per-frame update cost whenever $|\Delta_t| \ll |\mathcal{T}_t|$. The constant on `streaming_update` is six (the six edges per edited tetrahedron); the κ factor on `local_recompute` is the valence of touched candidates, which can be large in practice and is the source of the persistent-state benefit.

At a high level, `full_rebuild` revisits all active tetrahedra after every edit and therefore scales with the current assembled problem size. `local_recompute` restricts attention to candidate edges or matrix entries touched by the current event, but it still rescans all static incident tetrahedra needed to recompute those values exactly. `streaming_update` performs the least rework: it visits only the changed tetrahedra, updates the maintained hidden state or accumulated entry values, and then materializes the sparse matrix. In practice, our results show that this difference is most visible in the update path, while the remaining frame-time gap between exact local policies is increasingly governed by the solve and sparse-kernel costs once rebuild work has been removed.

3.6 Dynamic Connectivity

Our pipeline also tracks tetrahedron connectivity under the same event stream. Our implementation uses standard union-find with path compression and union-by-rank for active queries, but rebuild periodically from scratch from the current active mask rather than maintained incrementally. We choose this design over Tarjan’s incremental disjoint-set structure [Tarjan 1975], which does not natively support deletions, and over Holm et al.’s fully-dynamic exact connectivity [Holm et al. 2001], which does support arbitrary deletions but is substantially more involved to implement and benchmark cleanly. Periodic rebuild gives correctness for deletions (since each rebuild is computed from the current active mask) without the implementation overhead of a fully-dynamic structure, and connectivity queries are spot-checked against sampled breadth-first search sanity tests inside the same benchmark loop.

Algorithm 1 STA-FEM streaming update loop

Require: V (vertices), T (superset tetrahedra), active mask a_0
Ensure: A_t maintained exactly equivalent to rebuild at every frame

- 1: Initialize connectivity state from (V, T, a_0)
- 2: Initialize edge-multiplicity map c_0 and sparse matrix A_0
- 3: **for** $t = 0$ to $F - 1$ **do**
- 4: Receive edit sets Δ_t^- (deleted) and Δ_t^+ (added)
- 5: Update active mask and connectivity using $\Delta_t^- \cup \Delta_t^+$
- 6: **for all** $\tau \in \Delta_t^- \cup \Delta_t^+$ **do**
- 7: **for all** $e = (u, v) \in E(\tau)$ **do** ▷ 6 edges per tet
- 8: $c_t(e) += 1[\tau \in \Delta_t^+] - 1[\tau \in \Delta_t^-]$
- 9: **if** $c_t(e)$ transitions between 0 and > 0 **then**
- 10: Insert/remove off-diagonal entries
- 11: $A_t(u, v), A_t(v, u)$
- 12: Update diagonal degree terms $A_t(u, u), A_t(v, v)$
- 13: **end if**
- 14: **end for**
- 15: **end for**
- 16: Finalize sparse $A_t \leftarrow L_t + \varepsilon I$
- 17: Solve $A_t x_t = b_t$ via preconditioned CG
- 18: **end for**

3.7 Per-Frame Algorithm

Pseudocode for the overall algorithm for STA-FEM, run on each frame, is provided in Algorithm 1.

4 Implementation

Our implementation is organized around three components. First, an incremental tracker maintains edge counts and sparse updates for the binary-edge proxy, while a second pair of trackers maintains accumulated entry values for a vector-valued linear-elasticity transfer study. In both cases, `local_recompute` rescans only candidate entries touched by each event and `streaming_update` preserves maintained state across frames. Second, a periodic-rebuild connectivity module maintains dynamic component queries under the same event stream. Third, the benchmark driver executes matched schedules across modes, models, and scenarios while recording exact parity metrics against `full_rebuild`.

From an integration standpoint, STA-FEM is intended to replace only the per-frame topology-dependent assembly step inside an existing tetrahedral solver loop. The surrounding solve, preconditioner interface, and time-stepping logic can remain unchanged, provided the pipeline exposes the per-frame edit stream (Δ_t^-, Δ_t^+) over the preallocated candidate element pool. This covers practical regimes such as pre-tessellated fracture assets, offline-authored refinement hierarchies [Koschier et al. 2014], and scripted merge schedules, where candidate elements are known ahead of time even though only a subset is active per frame. Our numerical experiments use conjugate gradients with diagonal preconditioning.

5 Experimental Setup

5.1 Models, Scenarios, and Metrics

We perform numerical experiments using four tetrahedral objects from the dataset of Cutler et al. [2004]: (1) Bunny (10k, 50k, and

460k-element versions), (2) Gargoyle (50k elements), and Hand (100k elements). Each model is tested under three scripted topology-edit scenarios: **fracture** (delete tetrahedra inside an adaptively chosen slab); **refinement** (deactivate parent tetrahedra and activate refined children in a superset mesh); and **merge** (begin from a deleted slab and reinsert tetrahedra over time to reconnect components). For each experiment, we report several key quantitative metrics: average frame time; average CG solve time and iteration count; average matrix update time; exact matrix parity against rebuild, including mismatch count and maximum absolute sparse-entry difference; connectivity mismatch rate; and matrix sparsity mismatch frames when parity checking is enabled. Various tests compare the three policies introduced in Section 3.5.

5.2 Element-Assembled Elasticity Study

To test whether the maintenance idea extends beyond the proxy operator, we also run a transfer study on a vector-valued linear-tetrahedron elasticity matrix assembled from per-element 12×12 local blocks. This study uses Bunny 10k under the same fracture, refinement, and merge schedules, with 50 seeds and four frames per scenario. The comparison again uses `full_rebuild`, `exact_local_recompute`, and `exact_streaming_update`. We additionally run two follow-up diagnostics on Bunny 10K: a small implicit Euler dynamic loop for fracture and merge, and a repeated-locality elasticity diagnostic in which the same slab region is edited over multiple delete/add cycles, specifically to test when persistent state helps beyond one-shot local recomputation.

6 Results

6.1 Element-Assembled Elasticity Transfer

We open the results section with the elasticity transfer study because it provides the strongest non-proxy evidence in the paper and most directly speaks to standard FEM assembly. On Bunny 10K, both exact maintenance policies preserved zero elasticity-mismatch frames relative to rebuild in all 600 frame comparisons per policy, with the largest streaming-versus-rebuild entry difference remaining at machine precision (8.3×10^{-17}). Table 1 reports the 50-seed aggregate. This experiment as evidence that the maintenance pattern transfers to a block-structured element-assembled operator.

We highlight two points regarding this test. First, the same qualitative ordering survives on a true element-assembled operator: both exact local policies dramatically reduce frame time relative to global rebuild, and `streaming_update` again reduces update cost further. For Bunny 10k fracture, frame time drops from 1197.78 ms to 718.83 ms while update time drops from 535.89 ms to 0.78 ms—a roughly 690× reduction in update path cost. Second, the head-to-head frame-time ordering remains nuanced but favorable across all three scenarios, with the largest gap in refinement where persistent state avoids repeated rescans of many touched block entries.

6.2 Dynamic Elasticity Experiment

To connect the maintained operator more directly to a real FEM-style loop, we also ran small implicit Euler dynamic experiments on Bunny 10k fracture and merge. In this setting, each frame solves

$$(M_t + h^2 K_t) u_{t+1} = M_t (u_t + h v_t) + h^2 f, \quad (9)$$

Table 1. Linear-elasticity transfer study on Bunny 10K (mean over 50 seeds). Both exact policies preserve zero mismatches vs. rebuild. All times in ms; R = full rebuild, L = local recompute, S = streaming update.

Scenario	Frame time (ms) ↓			Update time (ms) ↓		
	R	L	S (ours)	R	L	S (ours)
Fracture	1197.78	754.63	718.83	535.891	28.346	0.778
Refinement	1276.24	1037.63	775.88	570.116	261.123	9.830
Merge	1198.28	759.01	719.40	536.661	33.750	0.799

Table 2. All-model comparison across all three policies (mean ± std over 50 independent seeds, diagonal preconditioner). R = full rebuild, L = local recompute, S = streaming update (ours). All times in ms. Bold marks the lowest mean per metric per row.

Model	Scenario	Frame time (ms) ↓			Update time (ms) ↓		
		R	L	S (ours)	R	L	S (ours)
Bunny 50k	Fracture	365.4 ± 20.5	231.0 ± 12.2	230.9 ± 11.8	138.1 ± 8.5	0.57 ± 0.15	0.41 ± 0.10
	Refinement	383.5 ± 20.7	246.5 ± 13.3	246.4 ± 14.1	144.1 ± 8.2	4.12 ± 0.14	3.45 ± 0.10
	Merge	366.0 ± 23.0	231.8 ± 12.6	230.6 ± 11.9	137.8 ± 9.7	0.53 ± 0.04	0.40 ± 0.02
Gargoyle 50k	Fracture	406.1 ± 15.8	265.3 ± 12.8	261.0 ± 9.4	143.2 ± 6.6	0.93 ± 0.06	0.65 ± 0.03
	Refinement	410.5 ± 9.7	283.4 ± 11.3	282.2 ± 12.0	143.8 ± 4.3	4.07 ± 0.15	3.39 ± 0.09
	Merge	399.5 ± 15.0	256.0 ± 5.6	261.3 ± 8.3	140.5 ± 6.4	0.87 ± 0.05	0.64 ± 0.02
Hand 100k	Fracture	1055.4 ± 41.5	769.4 ± 30.9	768.7 ± 30.1	297.1 ± 17.1	2.08 ± 0.10	1.39 ± 0.04
	Refinement	1111.2 ± 40.1	813.0 ± 29.4	809.4 ± 29.1	314.0 ± 16.0	8.62 ± 1.20	6.79 ± 0.15
	Merge	1054.0 ± 40.3	766.0 ± 29.1	766.8 ± 30.8	296.4 ± 16.4	1.99 ± 0.09	1.39 ± 0.04
Bunny 460k	Fracture	4671.1 ± 93.6	2892.6 ± 63.8	2923.8 ± 74.0	1770.7 ± 47.6	19.91 ± 14.07	10.75 ± 0.27
	Refinement	4968.5 ± 83.7	3093.5 ± 67.3	3108.2 ± 76.1	1890.7 ± 42.9	63.66 ± 1.41	50.70 ± 1.26
	Merge	4697.9 ± 93.2	2888.2 ± 71.6	2915.9 ± 76.5	1780.5 ± 44.4	15.47 ± 0.42	10.39 ± 0.25

where K_t is the maintained elasticity operator, M_t is a maintained lumped mass matrix, h is a fixed timestep, and f is a fixed external load. This formulation places the maintained assembly directly inside a time-stepping loop, where topology edits arrive mid-simulation and the maintained operator must remain valid for each successive solve.

The dynamic results are consistent with the rest of the paper. Across 50 seeds, both exact local policies again preserved zero mismatches relative to rebuild in both scenarios. For Bunny 10k fracture, full rebuild averaged 1213.07 ms per frame, `local_recompute` reduced that to 774.62 ms, and `streaming_update` reduced it further to 739.71 ms; update cost dropped from 534.57 ms under rebuild to 28.12 ms under `local_recompute` and to 0.86 ms under `streaming_update`. For Bunny 10k merge, full rebuild averaged 1214.25 ms per frame, `local_recompute` reduced that to 781.84 ms, and `streaming_update` reduced it further to 740.25 ms; update cost dropped from 534.40 ms to 33.38 ms and then to 0.87 ms. These two dynamic scenarios support the practical integration claim: the maintained-assembly idea still matters once the operator sits inside a simple dynamics loop.

6.3 Multi-Model Results

Having established the elasticity and dynamic-loop results, we now turn to the broader proxy-operator evidence. Table 2 summarizes results across all four objects, three scenarios, and all three policies, with mean ± std over 50 seeds per configuration. Across all models and scenarios, `streaming_update` improves end-to-end frame time relative to `full_rebuild`. The observed speedups range from 1.37× on Hand 100k to 1.61× on Bunny 460k merge.

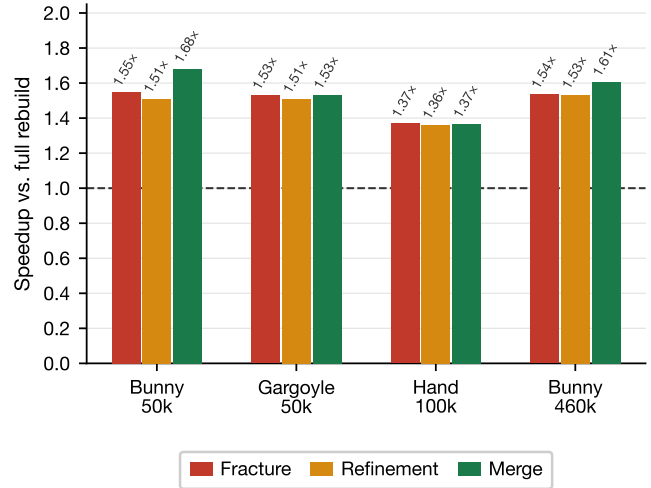


Fig. 2. Model speedup summary for STA-FEM versus the full rebuild policy. Streaming updates improve end-to-end frame time across all tested scenarios and objects.

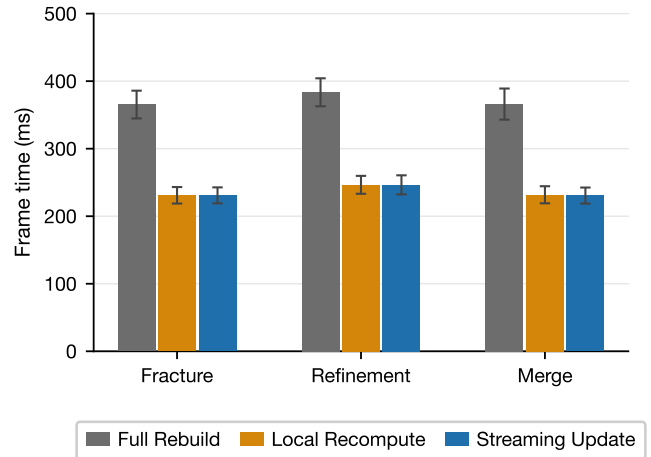


Fig. 3. Representative frame times for STA-FEM, local recompute, and full rebuild policies on the Bunny 50K model. We observe a consistent frame time reduction for `streaming_update` across fracture, refinement, and merge. Although update time is consistently best with `streaming_update`, overall frame time is statistically equivalent to the local recompute timings since the system update is a small part of the total frame time.

In addition to Table 2, which reports the full results of `streaming_update` compared to the `local_recompute` and `full_rebuild` policies, Figure 2 plots the speedup factors of our streaming approach versus the full rebuild strategy, while Figure 3 plots frame time for each method for each task on the Bunny 50k model. We stress that the only aspect of the solver loop that varies between these algorithms is system update: streaming reduces matrix update cost by 331× on Bunny 50k fracture, 226× on Gargoyle 50k fracture, and 173× on Bunny 460k fracture relative to full rebuild.

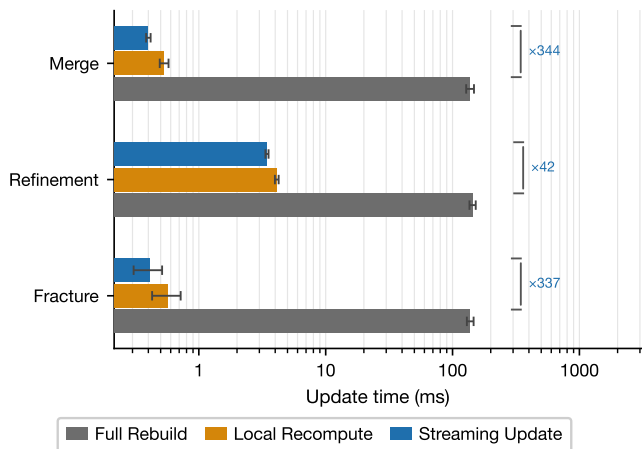


Fig. 4. Update costs for the Bunny 50K example. The proposed method nearly eliminates rebuild-path cost relative to the rebuild baselines.

Comparing the two exact local policies, `streaming_update` achieves lower update time than `local_recompute` in every single configuration—consistently by $1.2\times$ to $1.5\times$ —because persistent maintained state avoids rescanning incident tetrahedra on each frame. However, overall frame time differences between the two exact policies are smaller, since the rebuild cost is only part of the total frame time in the simulation. In cases where `local_recompute` shows a numerically lower mean frame time, the differences are well within one standard deviation and are not statistically distinguishable. The differences in update time, on the other hand, are statistically significant, which is the goal of our method. The results also illustrate that the larger the mesh is, the greater the advantage of our method.

6.4 Scaling and Memory Usage

A Bunny 10k fracture locality sweep shows that update cost scales with edit extent. When the deleted slab half-width increases from 0.01 to 0.08, the average update cost of `local_recompute` rises from 0.054 ms to 0.319 ms, while `streaming_update` rises from 0.042 ms to 0.224 ms. Both exact local policies therefore scale with event size, but the cost of STA-FEM remains consistently below exact local rescanning in this sweep.

The added state required by the persistent maintenance of STA-FEM remains modest in absolute terms and stays below the stronger `local_recompute` baseline in our implementation. For Bunny 50K, the estimated maintenance-state footprint is 0.048 MB for `full_rebuild`, 4.51 MB for `local_recompute`, and 3.86 MB for `streaming_update`. The same ordering holds for the Bunny 10K model. The streaming footprint is dominated by the persistent edge-multiplicity map and scales linearly with active tetrahedra; under 4 MB at Bunny 50k is small relative to typical FEM working sets.

6.5 Spatiotemporal Edit Locality

We conduct one further experiment to show when STA-FEM can be particularly advantageous. In this experiment, we repeatedly delete and reinsert tetrahedra inside the same slab region of the

Bunny 10k over eight frames, so the edited region remains local but recurs over time. In this regime, `local_recompute` still pays to rescan the same candidate block entries frame after frame, whereas `streaming_update` only applies incremental deltas. Across 50 seeds, `local_recompute` reduces average update time from 518.69 ms to 26.42 ms, while `streaming_update` reduces it further to 1.30 ms—a roughly $20\times$ gap between the two exact policies—with frame time falling from 680.29 ms to 649.66 ms.

6.6 When to Use STA-FEM

The above results suggest that STA-FEM is most beneficial when (i) the candidate element pool can be preallocated, (ii) per-frame assembly is a non-trivial fraction of frame time (visible at Bunny 50k and above on our hardware), and (iii) edits exhibit temporal locality, with the same regions touched repeatedly. For one-shot, well-separated edits of small meshes, exact local recomputation already removes most of the rebuild cost, and persistent state offers smaller marginal benefit in those cases (though it tends to perform at least as well as `local_recompute`).

7 Conclusion and Future Work

STA-FEM demonstrates that preplanned dynamic-topology tetrahedral simulation pipelines can maintain solver structure incrementally rather than rebuilding from scratch after every edit, with exact equivalence to rebuild at every frame by construction. The method delivers consistent end-to-end speedups for simulation frame time by reducing matrix update cost by orders of magnitude. Our results demonstrate that, in suitable settings, exact streaming assembly can be a practical and efficient aid for simulating dynamic tetrahedral meshes.

Future work could include integrating with system-level update methods such as AMPS [Yeung et al. 2020], investigating parallel processing of edits to improve performance, and integrating our algorithm with production FEM codebases.

Acknowledgments

D.H. was supported by NSF grant number 2450401.

References

- Kook Ahn, Sudipto Guha, and Andrew McGregor. 2012. Analyzing Graph Structure via Linear Measurements. In *Proceedings of the Twenty-Third Annual ACM-SIAM Symposium on Discrete Algorithms (SODA '12)*. SIAM, 459–467. doi:10.1137/1.9781611973099.40
- Douglas N. Arnold, Arup Mukherjee, and Luc Pouly. 2000. Locally Adapted Tetrahedral Meshes Using Bisection. *SIAM Journal on Scientific Computing* 22, 2 (2000), 431–448.
- Daniel Bielser, Pascal Glardon, Matthias Teschner, and Markus Gross. 2003. A State Machine for Real-Time Cutting of Tetrahedral Meshes. In *11th Pacific Conference on Computer Graphics and Applications, 2003. Proceedings. IEEE*, 377–386.
- Yanqing Chen, Timothy A. Davis, William W. Hager, and Sivasankaran Rajamanickam. 2008. Algorithm 887: CHOLMOD, Supernodal Sparse Cholesky Factorization and Update/Downdate. *ACM Trans. Math. Software* 35, 3, Article 22 (2008), 14 pages. doi:10.1145/1391989.1391995
- Rajesh Chitnis, Graham Cormode, Hossein Esfandiari, MohammadTaghi Hajiaghayi, Andrew McGregor, Morteza Monemizadeh, and Sofya Vorotnikova. 2016. Kernelization via Sampling with Applications to Dynamic Graph Streams. In *Proceedings of the Twenty-Seventh Annual ACM-SIAM Symposium on Discrete Algorithms (SODA '16)*. SIAM, 1326–1344. doi:10.1137/1.9781611974331.ch92
- Barbara Cutler, Julie Dorsey, and Leonard McMillan. 2004. Simplification and Improvement of Tetrahedral Models for Simulation. In *Proceedings of the 2004 Eurographics/ACM SIGGRAPH Symposium on Geometry Processing*, 93–102.
- Timothy A. Davis and William W. Hager. 1999. Modifying a Sparse Cholesky Factorization. *SIAM J. Matrix Anal. Appl.* 20, 3 (1999), 606–627. doi:10.1137/S0895479897321076
- Linxu Fan, Floyd M. Chitalu, and Taku Komura. 2022. Simulating Brittle Fracture with Material Points. *ACM Transactions on Graphics* 41, 5 (2022). doi:10.1145/3522573
- Joan Feigenbaum, Sampath Kannan, Andrew McGregor, Siddharth Suri, and Jian Zhang. 2005. On Graph Problems in a Semi-Streaming Model. *Theoretical Computer Science* 348, 2 (2005), 207–216. doi:10.1016/j.tcs.2005.09.013
- Automata, Languages and Programming: Algorithms and Complexity (ICALP-A 2004).
- Zachary Ferguson, Teseo Schneider, Danny M. Kaufman, and Daniele Panozzo. 2023. In-Timestep Remeshing for Contacting Elastodynamics. *ACM Transactions on Graphics* 42, 4, Article 145 (2023). doi:10.1145/3592428
- David Hahn and Chris Wojtan. 2015. High-Resolution Brittle Fracture Simulation with Boundary Elements. *ACM Transactions on Graphics* 34, 4, Article 151 (2015), 12 pages. doi:10.1145/2766896
- Jacob Holm, Kristian de Lichtenberg, and Mikkel Thorup. 2001. Poly-Logarithmic Deterministic Fully-Dynamic Algorithms for Connectivity, Minimum Spanning Tree, 2-Edge, and Biconnectivity. *J. ACM* 48, 4 (2001), 723–760. doi:10.1145/502090.502095
- Michael Kapralov, Yin Tat Lee, Cameron Musco, Christopher Musco, and Aaron Sidford. 2015. Single Pass Spectral Sparsification in Dynamic Streams. arXiv:1407.1289 [cs.DS] <https://arxiv.org/abs/1407.1289>
- Dan Koschier, Sebastian Lipponer, and Jan Bender. 2014. Adaptive Tetrahedral Meshes for Brittle Fracture Simulation. In *Proceedings of the ACM SIGGRAPH/Eurographics Symposium on Computer Animation (SCA '14)*. Eurographics Association, 57–66. doi:10.2312/sca.20141123
- Igor Kossaczky. 1994. A Recursive Approach to Local Mesh Refinement in Two and Three Dimensions. *J. Comput. Appl. Math.* 55, 3 (1994), 275–288. doi:10.1016/0377-0427(94)90034-5
- Joseph M. Maubach. 1995. Local Bisection Refinement for n -Simplicial Grids Generated by Reflection. *SIAM Journal on Scientific Computing* 16, 1 (1995), 210–227.
- Andrew McGregor. 2014. Graph Stream Algorithms: A Survey. *ACM SIGMOD Record* 43, 1 (2014), 9–20. doi:10.1145/2627692.2627694
- William F Mitchell. 2016. 30 Years of Newest Vertex Bisection. In *AIP Conference Proceedings*, Vol. 1738. AIP Publishing LLC, 020011.
- Neil Molino, Zhaosheng Bao, and Ronald Fedkiw. 2004. A Virtual Node Algorithm for Changing Mesh Topology During Simulation. *ACM Transactions on Graphics* 23, 3 (2004), 385–392. doi:10.1145/1015706.1015734
- Matthias Müller, Nuttapong Chentanez, and Tae-Yong Kim. 2013. Real Time Dynamic Fracture with Volumetric Approximate Convex Decompositions. *ACM Transactions on Graphics* 32, 4 (2013), 1–10.
- Shan Muthukrishnan. 2005. Data Streams: Algorithms and Applications. *Foundations and Trends in Theoretical Computer Science* 1, 2 (Aug. 2005), 117–236. doi:10.1561/0400000002
- James F. O'Brien and Jessica K. Hodgins. 1999. Graphical Modeling and Animation of Brittle Fracture. In *Proceedings of the 26th Annual Conference on Computer Graphics and Interactive Techniques (SIGGRAPH '99)*. Association for Computing Machinery, New York, NY, USA, 137–146. doi:10.1145/311535.311550
- Silvia Sellán, Jack Luong, Leticia Mattos Da Silva, Aravind Ramakrishnan, Yuchuan Yang, and Alec Jacobson. 2023. Breaking Good: Fracture Modes for Realtime Destruction. *ACM Transactions on Graphics* 42, 1 (2023), 1–12.
- Eftychios Sifakis and Jernej Barbič. 2012. FEM Simulation of 3D Deformable Solids: A Practitioner's Guide to Theory, Discretization and Model Reduction. In *ACM SIGGRAPH 2012 Courses (SIGGRAPH '12)*. Association for Computing Machinery, New York, NY, USA, Article 20, 50 pages. doi:10.1145/2343483.2343501
- Robert Endre Tarjan. 1975. Efficiency of a Good But Not Linear Set Union Algorithm. *J. ACM* 22, 2 (1975), 215–225. doi:10.1145/321879.321884
- Martin Wicke, Daniel Ritchie, Bryan M. Klingner, Sebastian Burke, Jonathan R. Shewchuk, and James F. O'Brien. 2010. Dynamic Local Remeshing for Elastoplastic Simulation. *ACM Transactions on Graphics* 29, 4, Article 49 (2010), 11 pages. doi:10.1145/1778765.1778786
- Yu-Hong Yeung, Alex Pothen, and Jessica Crouch. 2020. AMPS: A Real-Time Mesh Cutting Algorithm for Surgical Simulations. *Concurrency and Computation: Practice and Experience* 32, 17 (2020), e5500. doi:10.1002/cpe.5500
- Behrooz Zarebavani, Danny M. Kaufman, David I. W. Levin, and Maryam Mehri Dehnavi. 2025. Adaptive Algebraic Reuse of Reordering in Cholesky Factorizations with Dynamic Sparsity Patterns. *ACM Transactions on Graphics* 44, 4 (2025). doi:10.1145/3731179